International Journal of Refractory Metals and Hard Materials 112 (2023) 106142

Contents lists available at ScienceDirect

International Journal of Refractory Metals and Hard Materials

journal homepage: www.elsevier.com/locate/IJRMHM

Gravitational mass flow measurements of various granular materials in relation to an extended Bond number

M. Just [a,b], A. Medina Peschiutta [a,b], F. Hippe [a], R. Useldinger [a], J. Baller [b,*]

[a] CERATIZIT Luxembourg S.à r.l., 101 Route de Holzem, L-8232, Luxembourg
[b] Department of Physics & Materials Science, University of Luxembourg, 1511 Luxembourg, Luxembourg

ARTICLE INFO

Keywords:
Granular flowability
Beverloo law
Angle of repose
Granular bond number
RTP-powder
Cemented carbides

ABSTRACT

Uniaxial die pressing is a commonly used shaping technique in powder metallurgy. The initial step within the compression cycle is the filling process of the cavity with granular materials. Here, the goal is to have a reproducible cavity filling to manufacture compressed parts of consistent quality. Besides effects linked to the geometry of the cavity and the mechanisms of filling, the flowability of the granular material plays a major role. Therefore, a deeper understanding of the flow behaviour is in the centre of the present study. In order to assess the flowability, two different experimental methods are used. Granular materials of the same composition but different granular size distributions are characterised by angle of repose (AOR) and mass flow rate measurements. The two methods deliver a set of parameters that are compared using the granular Bond number. Based on the empirical findings, a modification of the granular Bond number is suggested.

1. Introduction

In the powder metallurgy industry, it is common to wet-mill the components and spray-dry the resulting homogeneous slurry. The obtained granules are referred to as ready-to-press (RTP) powders. RTP powders are often used in combination with automatic uniaxial presses, where a filling shoe containing the granules passes over the die and fills the cavity. Many factors influence the die-filling process: die geometry [1], humidity of the powder [2], filling shoe geometry [3] and last but not least, the flowability of the powder [4,5]. Two well-known techniques to characterise the flow properties are the angle of repose (AOR) and gravitational mass flow measurements.

In order to measure the AOR, the granular material is poured on a horizontal plane, creating a pile with a conical shape. The angle between the inclined surface of the piled-up material and the horizontal base plane constitutes the AOR [6]. The shape and size of the pile relate to powder properties such as particle size [7], particle morphology [8] and interparticle forces [9]. Moreover, the literature suggests that a low AOR is preferable as it implies excellent flow properties [10,11]. Consequently, the fundamental parameters influencing the AOR also affect granular flow.

Elekes and Parteli [9] recently studied the effect of interparticle attraction on the shape of the pile using numerical methods. The results show an increasing AOR with increasing interparticle attraction. Elekes and Parteli [9] describe the effect of the interparticle attraction by using the granular Bond number (Bo), which is the ratio between the maximum interparticle attractive force and the gravitational force F_g. Castellano [12] describes the granular Bond number, assuming the dominant attractive forces between fine dry powders to be van der Waals forces F_{vdW}:

$$Bo = \frac{F_{vdW}}{F_g} \tag{1}$$

However, for powders of different natures, supplementary forces such as electrostatic forces, capillary forces, and solid contact bridges have also to be considered [13–15]. Generally, the smaller the particle diameter, the higher the granular Bond number and the higher the AOR. Geldart et al. [16], Lumay et al. [17] and Just et al. [18] have reported similar results.

Furthermore, Elekes and Parteli [9] describe the relationship between the granular Bond number and the static AOR θ_r from simulations as follows (in radians):

$$\theta_r \approx tan^{-1}\left(\mu_{eff,\infty} * \left(1 + \beta^* \sqrt{Bo}\right)\right) \tag{2}$$

here, $\mu_{eff,\infty}$ is the infinite effective friction coefficient for a class of

* Corresponding author.
E-mail address: joerg.baller@uni.lu (J. Baller).

https://doi.org/10.1016/j.ijrmhm.2023.106142
Received 13 October 2022; Received in revised form 20 January 2023; Accepted 25 January 2023
Available online 28 January 2023

Table 1
Selected samples and their properties, data in columns marked with "*" are from [18]. Errors stem from repeated measurements.

Sample code*	Sieving Class*	Sauter diameter $d_{[2,3]}$ (μm)*	Bulk density (g/cm³)*	Tap density (g/cm³)*	H (−)*	Pyc. density (g/cm³)*	Bo($d_{[2,3]}$) (−) *Error: 100% (see text)*
S	Standard	159 ± 4	3.36 ± 0.01	3.66 ± 0.01	1.09 ± 0.01	11.50 ± 0.01	0.04
A1	>224	241 ± 2	3.26 ± 0.01	3.51 ± 0.01	1.08 ± 0.01	11.50 ± 0.01	0.02
A2	200–224	212 ± 1	3.27 ± 0.01	3.51 ± 0.01	1.07 ± 0.01	11.52 ± 0.01	0.02
A3	150–200	170 ± 1	3.28 ± 0.01	3.53 ± 0.01	1.08 ± 0.01	11.52 ± 0.01	0.03
A4	125–150	127 ± 1	3.28 ± 0.01	3.54 ± 0.01	1.08 ± 0.01	11.52 ± 0.01	0.06
A5	<125	54 ± 1	3.37 ± 0.01	3.66 ± 0.01	1.09 ± 0.01	11.53 ± 0.01	0.30
A6	100–125	104 ± 1	3.29 ± 0.01	3.55 ± 0.01	1.08 ± 0.01	11.52 ± 0.01	0.08
A7	63–100	79 ± 1	3.30 ± 0.01	3.58 ± 0.01	1.09 ± 0.01	11.52 ± 0.01	0.14
B1	125–200	161 ± 1	3.30 ± 0.01	3.56 ± 0.01	1.08 ± 0.01	11.51 ± 0.01	0.03
B2	150–224	177 ± 3	3.27 ± 0.01	3.52 ± 0.01	1.08 ± 0.01	11.52 ± 0.01	0.03
C1	125–224	165 ± 3	3.29 ± 0.01	3.55 ± 0.01	1.08 ± 0.01	11.51 ± 0.01	0.03

materials, and annotation r marks the static AOR θ. It is independent of physical interactions of cohesive nature and contains all other influences on the AOR θ, e.g. morphology and roughness. Furthermore, β is a weighting factor for the impact of the granular Bond number on the AOR θ_r.

Another method to assess the flowability of powders is the measurement of, gravitational mass flow rate; such tests can be performed with a Hall-Flow Meter as described in ASTM B213 [19]. Anand et al. [20] correlated the Bond number with the mass flow rate for wet cohesive powders (particles smaller than 100 μm) via discrete element method (DEM) simulations. They propose considering the granular Bond number in the fitting parameter k of the classical empirical model of Beverloo et al. [21].

Initial investigations of Beverloo et al. [21] with organic materials and a flat-bottomed hopper yielded the so-called Beverloo Law, which enables the prediction of the mass flow rates in accordance to

$$\dot{m} = C^* \rho_{app}{}^* \sqrt{g}^* \sqrt{(D - k^* d_p)^5} \tag{3}$$

here, ρ_{app} is the apparent density, also known as the bulk density, g represents the gravitational acceleration, D corresponds to the orifice diameter, and d_p is the diameter of the granules. C and k are fitting parameters, ranging for C from 0.55 to 0.65 and k from 1 to 3 [21].

Recently, the effect of the granular Bond number has been increasingly considered within the last years in experimental studies and simulations to describe the flowability and packing phenomena of granular materials [13,22]. For instance, Siliveru et al. [23] used the granular Bond number to predict the flow properties of a mixture of three different granular materials. Increasing the proportion of very fine powders (< 45 μm) within the mixture affects the flow behaviour negatively.

This paper proposes an extension of the granular Bond number considering the effect of friction that is not due to van der Waals forces. The friction coefficient is determined from AOR measurements, which are related to the mass flow rate of the RTP powders through orifices. The results are discussed in relation to the fitting parameters C and k in the Beverloo law.

2. Experimental

The upcoming sections provide detailed information about the properties of the selected granular materials, followed by an explanation of the measurement procedures for the mass flow rate ṁ (Beverloo law) and the AOR θ.

2.1. Granular samples with different properties

Table 1 summarises the properties of the selected hard metal RTP powders. The samples considered in this study consist of homogenised tungsten carbide, cobalt and organic binder. They are named using the following systematics: S ("standard") represents the unsieved mother batch from which all other samples are retrieved. The A-series represents different sieving fractions of S having narrower granule size distributions compared to the B-series. For example, C1 is produced by sieving S with the smallest (125 μm) and broadest (224 μm) mesh. The granular size distributions were measured with a laser diffraction system (Mastersizer 3000 by Malvern Panalytical). The Sauter mean diameter $d_{[2,3]}$ is the surface-volume mean diameter of a polydisperse system [24]. For instance, this parameter is widely used in literature; for example, one use is to describe the mean size of droplets of atomised fuel liquids [25] or sediments [26]. In our case, the Sauter mean diameter is used to express the mean diameter for each sample. A more detailed description of the samples, including granular size distributions, is given in Table 1 and our previous work [18].

The apparent density ρ_{app} and tap density ρ_{tap} was measured with the GranuPack-system [17] from Granutools, Belgium. The device measures the powder height for a given mass and calculates the apparent density. The tap densities were acquired by mechanical agitation (500 taps) of the selected granular material; the results are reported in Table 1. The Hausner ratio H expresses the ratio between both densities (ρ_{tap} / ρ_{app}) and is also used to classify powder and granular flowability. The pycnometer density ρ_{pyc} of the granules was measured with the Accupyc II 1340 from Micromeretics using Helium as measurement gas.

The granular Bond number describes the relationship between van der Waals forces F_{vdW} and the weight of a single granule. The van der Waals forces of dry granular materials are determined according to

$$F_{vdW} = \frac{A}{12^* z_0^2} \left(\frac{d_1{}^* d_2}{d_1 + d_2} \right) \tag{4}$$

where A is the Hamaker constant, z_0 is the closest distance between two spheres of diameters d_1 and d_2 [27] (typically z_0 = 4 nm [28]). Furthermore, Xie [29] extended Eq. (4) by considering surface

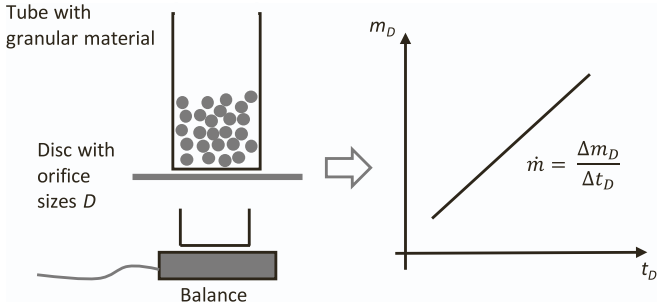

Fig. 1. Sketch of the device for measuring the mass flow rate $\dot{m}$ (left) and obtained data (right).

asperities, which showed an impact on the van der Waals forces, accounting for finer particles situated on the surface of bigger host particles. In this work, the particles are assumed to be spherical and dense, i. e. without intragranular porosity. Additionally, the presence of finer particles on the host surfaces is not considered.

The Hamaker constant for the granular systems in Table 1 was determined using atomic force microscopy (Veeco Multimode with NanoScope V Controller). This technique can directly measure the attractive forces between two bodies. The goal was to measure the attraction forces between a flat surface and a granule. This was achieved by attaching a single granule to a tipless silicon cantilever (from BudgetSensors). The cantilever has a nominal stiffness constant of 0.2 N/m and a nominal resonance frequency of 15 kHz. The flat surface was produced by compressing granules. The pull-off force is linked to the attractive forces and was measured between the granule and the flat surface. The measurements have been performed in nitrogen atmosphere in order to reduce the influence of humidity.

Two cantilevers were prepared as described above. The granule attached to it had different diameters of 187 ± 2 µm and 113 ± 1 µm respectively. The pull-off force (maximal force) was measured in contact mode on the flat surface for each of them at twenty different locations. The Hamaker constant was determined from each set of measurements as described by Israelachvili [30]. It turned out that the Hamaker constant differed from (1.5 ± 0.2) 10^{-22} J to (3.2 ± 0.7) 10^{-22} J for the two granule diameters. We attribute these differences mainly to the interplay between granule diameter and roughness of the flat surface. Moreover, the multi-component nature (WC, Co and organic binder) of the material, deviation of the stiffness of the two cantilevers from the nominal values given by the manufacturer and possible difference of the exact location of the glued granules on the two cantilevers lead to more uncertainties in the determination of the Hamaker constant. For the following, we therefore assume that the Hamaker constant in the order of 2 10^{-22} J with an error of 100%. This value is considered for the calculation of the granular Bond number.

The diameters d_1 and d_2 in Eq. (4) are assumed to be equal and are represented by the Sauter mean diameter $d_{[2,\,3]}$, which is used in literature for granular materials [23,31]. The calculated granular Bond numbers are presented in Table 1.

2.2. Measurement of the gravitational mass flow rate

The mass flow rate of the selected granular materials has been measured with the GranuFlow measuring system from Granutools (Fig. 1). The device consists of a cylindrical tube placed upon a metallic disc with various circular orifice diameters ranging from 1 to 8 mm. Below the orifice, a strain gauge is used as a balance to track the mass change. The mass flow rate $\dot{m}$ is measured at least three times for each orifice size.

Table 2
Measured AOR θ and friction coefficient µ, data in columns marked with "*" are from [18].

Sample	AOR θ (°)*	Friction coefficient µ (–)
S	34.3 ± 0.3	0.681 ± 0.008
A1	31.6 ± 0.2	0.614 ± 0.005
A2	31.8 ± 0.2	0.619 ± 0.005
A3	32.6 ± 0.2	0.640 ± 0.005
A4	32.9 ± 0.2	0.645 ± 0.005
A5	37.4 ± 0.3	0.765 ± 0.008
A6	32.9 ± 0.2	0.649 ± 0.005
A7	34.2 ± 0.1	0.680 ± 0.003
B1	32.5 ± 0.3	0.637 ± 0.007
B2	31.0 ± 0.2	0.602 ± 0.005
C1	32.0 ± 0.2	0.623 ± 0.005

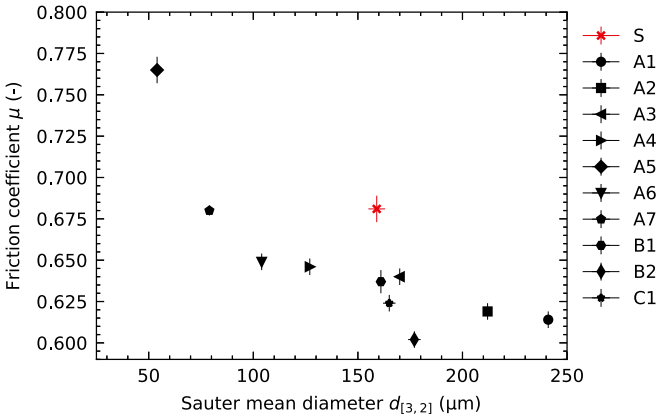

Fig. 2. The friction coefficient μ in dependency of the Sauter mean diameter $d_{[2,\,3]}$. Note that if error bars are not visible, they are smaller than the symbol size.

2.3. The angle of repose of granular materials

The AOR θ is measured using a new approach described in detail in [18]. The method determines the angle formed between the cone surface and the supporting plate while the granules are discharging from the hopper. First, the cone angle is calculated using an image processing algorithm. Next, several cone angles are determined by changing the base plate position below the funnel. With these values, the AOR θ is calculated as described by Just et al. [18]. Table 2 presents the calculated AORs θ and the friction coefficients µ. The friction coefficient µ is calculated with

$$\mu = tan(\theta) \tag{5}$$

in radians and is shown in Table 2.

3. Results and discussion

In this section, the relations between the friction coefficient, the granular Bond number, AOR and the mass flow rate are presented. This opens the discussion about an extended granular Bond number.

3.1. Relation between friction coefficient and particle size

Fig. 2 shows the friction coefficient calculated from the AOR θ with Eq. (5) in dependency of the Sauter mean diameter $d_{[2,\,3]}$ from Table 2. It is visible that the friction coefficient increases with decreasing particle diameter. Since a high AOR θ also results in a high friction coefficient µ, our result is in alignment with the findings of Lumay et al. [17], who report a substantial increase of the AOR θ for very fine particles below 100 µm.

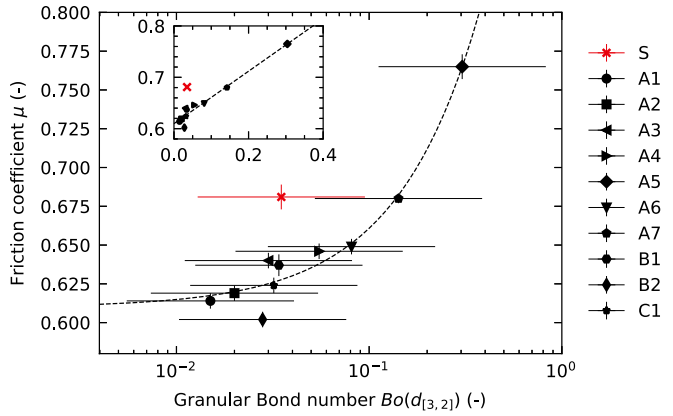

Fig. 3. The friction coefficient μ for various granules with respect to the calculated granular Bond number $Bo(d_{[2,\ 3]})$. Inset shows data with a linear scale.

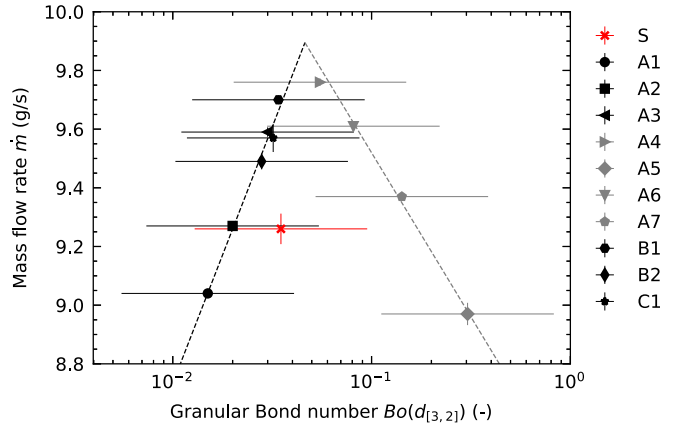

Fig. 4. Mass flow rate $\dot{m}$ through an orifice with a diameter of 5 mm in dependency on the granular Bond number $Bo(d_{[2,\ 3]})$ for all granular materials listed in Table 2. The dashed lines are power fits (additional information in Section 3.3). Note that if y error bars are not visible, they are smaller than the symbol size.

3.2. Relation between granular Bond number and friction coefficient

Fig. 3 displays the friction coefficient μ in dependency on the (logarithmic) granular Bond number. The findings show a linear relationship between the Bond number and the measured friction coefficient μ (for clarity, see also inset in Fig. 3). The dashed line in both graphs represents a linear fit according to

$$\mu = \mu_{eff,\infty} + const^{*}Bo \tag{6}$$

with $\mu_{eff,\infty} = 0.6$. Since the standard sample S has a much wider granular size distribution than the other samples, it has not been considered for the fit. Elekes and Parteli [9] calculated the influence of a broad range of granular Bond numbers between 10^{-6} to 10^{5} on the AOR θ by numerical simulations. Their findings state a strong increase of the AOR θ and thus the friction coefficient μ for granular Bond numbers higher than 10^{2}. In the present experimental study, the granular Bond numbers vary between 10^{-2} and 10^{0} for the samples listed in Table 1. Therefore, the representation of the friction coefficient as a function of the Bond number shown in Fig. 3 shows only part of the broad range of calculated friction coefficients found in [9]. In these limits, the presented experimental findings coincide well with the analysis of Elekes and Parteli [9].

Furthermore, Elekes and Parteli [9] showed that the influence of the attractive forces reduces significantly with an increase of the particle size d, i.e. the Bond number decreases, leading to an infinite effective friction coefficient $\mu_{eff,\infty}$ for granular Bond numbers below 10^{-1}. Below this granular Bond number, the friction coefficient μ, i.e. the AOR θ is nearly constant. The same can be observed for our experimental data (Fig. 3), described by the applied linear fit (Eq. (6)), also yielding an infinite friction coefficient $\mu_{eff,\infty}$. The absolute value of the infinite friction coefficient $\mu_{eff,\infty}$ is influenced by the granules' detailed composition, such as the amount or type of tungsten carbide.

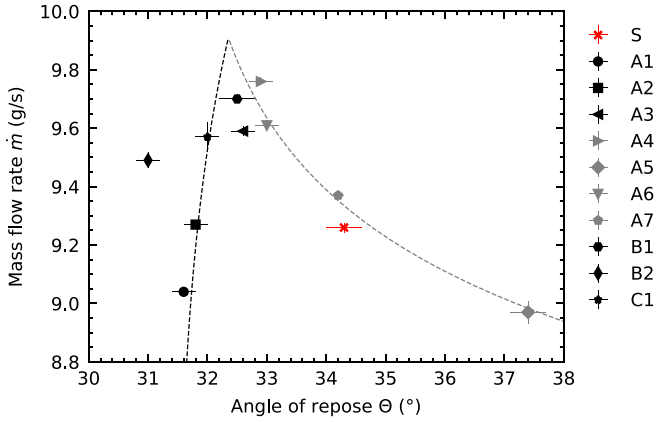

Fig. 5. Mass flow rate $\dot{m}$ through an orifice with a diameter of 5 mm in the function of the AOR θ for all granular materials listed.

3.3. The mass flow rate of granular materials as a function of the Bond number

Fig. 4 shows mass flow rates measured with an orifice diameter of 5 mm in function of the Bond number for all granules listed in Table 1. A similar trend was obtained using different orifice diameters (to be published). From Fig. 4, an increasing mass flow rate (A1, A2, B2, A3, C1, B1, black symbols) can be observed, followed by a decrease in mass flow rates (A4, A6, A7, A5, grey symbols) in function of the Bond number. According to Table 1, the increase in the Bond number is mainly due to a decrease in the mean particle diameter for samples A1, …, B1, A4, …, A5. Furthermore, two power law fits are inserted in Fig. 4 to determine an intersection point representing the Bond number for which the maximal possible mass flow rate for the considered granular system can be reached. Two opposing dependencies can explain the existence of a maximum in the mass flow rate: on the one hand, decreasing particle diameters (and thus increasing Bond numbers) lead to a higher mass flow rate through an orifice with a given size D (Eq. (3)). On the other hand, if the particle diameter reduces to values where the interparticle forces become dominant over gravitational forces (compare Eqs. (1) and (4)), the effective particle diameter increases due to formation of agglomerates and thus the mass flow rate is reduced. A similar relationship between granular size and cohesive effect expressed by the granular Bond number has been reported by Lu et al. [32].

The variation of the AOR with the granular Bond number is significantly bigger (approximately 20%, Table 2) than the variation of the mass flow rate (about 10%, Fig. 4). The reason is the gravitational force, which acts in AOR measurements only as a downhill force, i.e. the relatively weak van der Waals forces have a more significant influence. Whereas for the mass flow measurements, the gravitational force acts directly in the vertical direction and consequently, the van der Waals forces are thought to have a less pronounced effect. According to the literature [11], powders and granular materials with a Hausner ratio between 1.00 and 1.11 are considered to have excellent flowability. Following this criterion, all the reported materials have excellent flowability.

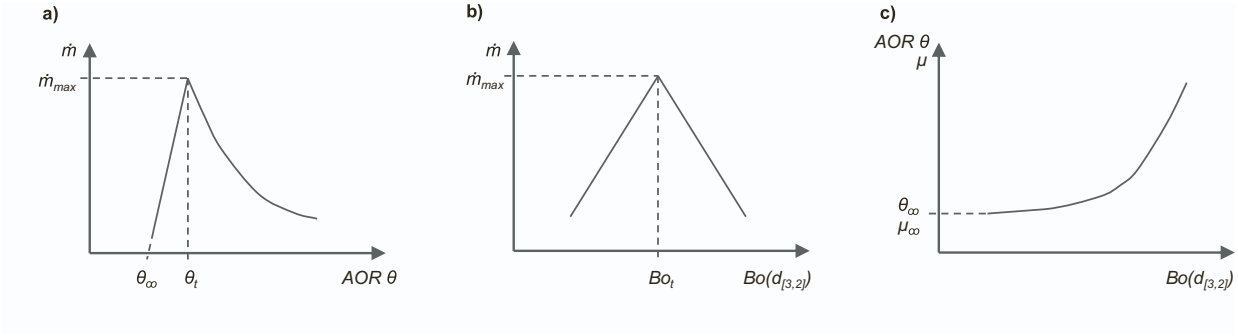

Fig. 6. Schematic results from (a) Fig. 5, (b) Fig. 4 and (c) Fig. 3.

3.4. The mass flow rate of granular materials as a function of the AOR

Fig. 5 shows the mass flow rate measured with an orifice diameter of 5 mm with respect to the AOR θ from Table 2. The data points were classified into the two categories used in Fig. 4. The dashed lines represent the mass flow rates in function of their corresponding AOR θ calculated using the trend lines shown in Fig. 4 and a linear fit generated by the data shown in Tables 1 & 2 (θ = f(Bo), figure not shown in this paper). This approach has been used for the two data categories (Bo < intersection point and Bo > intersection point in Fig. 4). The intersection point of the dashed lines represents the maximal mass flow rate (θ ≈ 32.4°). Low AORs θ typically indicate good flowability. Nevertheless, as already discussed in the previous paragraph, the opposite dependency of the mass flow rate from particle diameter and interparticle forces leads to a maximum mass flow rate; this effect is represented in Fig. 5.

3.5. The extended granular Bond number

A schematic comparison of Figs. 3, 4 and 5 is provided in Fig. 6 to illustrate the two opposite phenomena affecting the granular mass flow rate. First, for very low AOR θ, as the AOR θ increases, the mass flow rate increases until the maximal mass flow rate $\dot{m}_{max}$ is reached at AOR θ_t (Fig. 6a). This is mainly linked to the diminishing particle size with increasing Bond number. Then, above AOR θ_t, interaction forces or any other forces (see below) which hinder the free flow of particles start to take a considerable effect, leading to a decrease in the mass flow rate beyond AOR θ_t (Fig. 6a). Similar results can be found for the dependency of the mass flow rate ṁ from the Bond number (Fig. 6b).

As already stated, the granular Bond number pictures the comparison between interaction forces (here: only van der Waals forces) and the gravitational force. However, the position of the maxima in Fig. 6a and b results from the competition between decreasing particle diameter and increasing hindrance of particle flow. This hindrance can be due to van der Waals forces directly between the particles or geometrical constraints such as non-spherical particle shape, satellites on particle surfaces, humidity, etc. In addition, the influence of the particle size, surface roughness and cohesive effects has been shown by Anand et al. [20] and Lu et al. [32] to negatively affect the flow.

Therefore, we propose an extension of the granular Bond number such as $Bo_{ex} = \delta\, Bo$ to obtain $Bo_{ex} = 1$ at the position of the maximum in the mass flow rates. This scaling will affect the dependency of the AOR θ from the extended Bond number, i.e. the curve in Fig. 6c will be horizontally shifted, but the infinite friction coefficient $\mu_{eff,\infty}$ will not be affected. This is because $\mu_{eff,\infty}$ (and thus also the fitting parameters C and k in the Beverloo law, Eq. (3)) already contains all influences which hinder the flow of particles, not only the direct interaction forces (e.g. van der Waals forces). In this sense, $\mu_{eff,\infty}$ and Bo_{ex} refer to a similar collection of influences that hinder particles' flow. It goes beyond the scope of this analysis to discern if the scaling of the granular Bond number applies to other hard metal granules. This will be the subject of further studies.

4. Conclusion

During this study, mass flow rate and AOR measurements of a class of hard metal powders have been analysed. It turns out that all influences, which hinder the flow of particles, affect two main parameters of the experimental studies: the granular Bond number at which the mass flow through an orifice is maximal and the infinite friction coefficient. The infinite friction coefficient already pictures all influences on the particle flow, not only direct interactions such as van der Waals forces. A scaling of the granular Bond number, i.e. an extended granular Bond number Bo_{ex}, for which $Bo_{ex} = 1$ at the maximum mass flow rate, takes the same influences which hinder particle flow into account. More granular materials need to be studied to analyse the use of a scaled granular Bond number.

CRediT authorship contribution statement

M. Just: Methodology, Software, Formal analysis, Investigation, Data curation, Writing – original draft, Writing – review & editing, Visualization, Funding acquisition. **A. Medina Peschiutta:** Software, Investigation, Data curation, Writing – original draft, Writing – review & editing, Visualization. **F. Hippe:** Formal analysis, Validation, Resources, Supervision. **R. Useldinger:** Conceptualization, Validation, Resources, Writing – original draft, Writing – review & editing, Supervision, Project administration, Funding acquisition. **J. Baller:** Conceptualization, Methodology, Validation, Writing – original draft, Writing – review & editing, Visualization, Supervision, Project administration, Funding acquisition.

Declaration of Competing Interest

The authors declare that they have no known competing financial interests or personal relationships that could have appeared to influence the work reported in this paper.

Data availability

Data will be made available on request.

Acknowledgements

This work was funded in whole, or in part, by the Luxembourg National Research Fund and by CERATIZIT Luxembourg S.à r.l. with two Industrial Fellowships grants. Grant acronyms and references are MEPFLOW [13320318] and RHAMEP [14187658].

References

[1] C. Wu, L. Dihoru, A.C.F. Cocks, The flow of powder into simple and stepped dies, Powder Technol. 134 (2003) 24–39, https://doi.org/10.1016/S0032-5910(03)00130-X.

[2] Z. Wu, Y. Wu, A. Zakhvatayeva, X. Wang, Z. Liu, M. Yang, Q. Zheng, C.-Y. Wu, Influence of moisture content on die filling of pharmaceutical powders, J. Drug Deliv. Sci. Technol. 78 (2022), 103985, https://doi.org/10.1016/j.jddst.2022.103985.
[3] L.C.R. Schneider, A.C.F. Cocks, A. Apostolopoulos, Comparison of filling behaviour of metallic, ceramic, hardmetal and magnetic powders, Powder Metall. 48 (2005) 77–84, https://doi.org/10.1179/003258905X37549.
[4] L.A. Mills, I.C. Sinka, Effect of particle size and density on the die fill of powders, Eur. J. Pharm. Biopharm. 84 (2013) 642–652, https://doi.org/10.1016/j.ejpb.2013.01.012.
[5] I.C. Sinka, A.C.F. Cocks, Evaluating the flow behaviour of powders for die fill performance, Powder Metall. 52 (2009) 8–11, https://doi.org/10.1179/174329009X441736.
[6] H.M.B. Al-Hashemi, O.S.B. Al-Amoudi, A review on the angle of repose of granular materials, Powder Technol. 330 (2018) 397–417, https://doi.org/10.1016/j.powtec.2018.02.003.
[7] W. Wang, J. Zhang, S. Yang, H. Zhang, H. Yang, G. Yue, Experimental study on the angle of repose of pulverized coal, Particuology. 8 (2010) 482–485, https://doi.org/10.1016/j.partic.2010.07.008.
[8] Z.Y. Zhou, R.P. Zou, D. Pinson, A.B. Yu, Angle of repose and stress distribution of sandpiles formed with ellipsoidal particles, Granul. Matter 16 (2014) 695–709, https://doi.org/10.1007/s10035-014-0522-4.
[9] F. Elekes, E.J.R. Parteli, An expression for the angle of repose of dry cohesive granular materials on earth and in planetary environments, Proc. Natl. Acad. Sci. 118 (2021), https://doi.org/10.1073/pnas.2107965118.
[10] M. Šimek, V. Grünwaldová, B. Kratochvíl, Comparison of compression and material properties of differently shaped and sized paracetamols, KONA Powder Part. J. 34 (2017) 197–206, https://doi.org/10.14356/kona.2017003.
[11] R.L. Carr, Evaluating flow properties of solids, Chem. Eng. 72 (1965) 163–168.
[12] A. Castellanos, The relationship between attractive interparticle forces and bulk behaviour in dry and uncharged fine powders, Adv. Phys. 54 (2005) 263–376, https://doi.org/10.1080/17461390500402657.
[13] M. Giraud, C. Gatumel, S. Vaudez, G. Bernard-Granger, J. Nos, T. Gervais, H. Berthiaux, Investigation of a granular Bond number based rheological model for polydispersed particulate systems, Chem. Eng. Sci. 228 (2020), 115971, https://doi.org/10.1016/j.ces.2020.115971.
[14] A.J. Forsyth, S. Hutton, M.J. Rhodes, Effect of cohesive interparticle force on the flow characteristics of granular material, Powder Technol. 126 (2002) 150–154, https://doi.org/10.1016/S0032-5910(02)00046-3.
[15] K. Kuwagi, T. Mikami, M. Horio, Numerical simulation of metallic solid bridging particles in a fluidized bed at high temperature, Powder Technol. 109 (2000) 27–40, https://doi.org/10.1016/S0032-5910(99)00224-7.
[16] D. Geldart, E.C. Abdullah, A. Hassanpour, L.C. Nwoke, I. Wouters, Characterization of powder flowability using measurement of angle of repose, China Particuol. 4 (2006) 104–107, https://doi.org/10.1016/s1672-2515(07)60247-4.
[17] G. Lumay, F. Boschini, K. Traina, S. Bontempi, J. Remy, R. Cloots, N. Vandewalle, Measuring the flowing properties of powders and grains, Powder Technol. 224 (2012) 19–27, https://doi.org/10.1016/j.powtec.2012.02.015.
[18] M. Just, A. Medina Peschiutta, F. Hippe, R. Useldinger, J. Baller, Determination of the angle of repose of hard metal granules, Powder Technol. 407 (2022), 117695, https://doi.org/10.1016/j.powtec.2022.117695.
[19] ASTM International, ASTM B213–13: Standard Test Methods for Flow Rate of Metal Powders Using the Hall Flowmeter Funnel, ASTM Int, 2013.
[20] A. Anand, J.S. Curtis, C.R. Wassgren, B.C. Hancock, W.R. Ketterhagen, Predicting discharge dynamics of wet cohesive particles from a rectangular hopper using the discrete element method (DEM), Chem. Eng. Sci. 64 (2009) 5268–5275, https://doi.org/10.1016/j.ces.2009.09.001.
[21] W.A. Beverloo, H.A. Leniger, J. van de Velde, The flow of granular solids through orifices, Chem. Eng. Sci. 15 (1961) 260–269, https://doi.org/10.1016/0009-2509(61)85030-6.
[22] A. Singh, V. Magnanimo, K. Saitoh, S. Luding, Effect of cohesion on shear banding in quasistatic granular materials, Phys. Rev. E 90 (2014), 022202, https://doi.org/10.1103/PhysRevE.90.022202.
[23] K. Siliveru, C.G. Jange, J.W. Kwek, R.P.K. Ambrose, Granular bond number model to predict the flow of fine flour powders using particle properties, J. Food Eng. 208 (2017) 11–18, https://doi.org/10.1016/j.jfoodeng.2017.04.003.
[24] P.B. Kowalczuk, J. Drzymala, Physical meaning of the sauter mean diameter of spherical particulate matter, Part. Sci. Technol. 34 (2016) 645–647, https://doi.org/10.1080/02726351.2015.1099582.
[25] M. Volz, P. Habisreuther, N. Zarzalis, Correlation for the sauter mean diameter of a prefilmer airblast atomizer at varying operating conditions, Chemie-Ingenieur-Technik. 89 (2017) 320–327, https://doi.org/10.1002/cite.201600007.
[26] L. Filippa, A. Trento, A.M. Álvarez, Sauter mean diameter determination for the fine fraction of suspended sediments using a LISST-25X diffractometer, Meas. J. Int. Meas. Confed. 45 (2012) 364–368, https://doi.org/10.1016/j.measurement.2011.11.009.
[27] H.C. Hamaker, The London-van der Waals attraction between spherical particles, Physica. 4 (1937) 1058–1072, https://doi.org/10.1016/S0031-8914(37)80203-7.
[28] H. Krupp, Particle adhesion theory and experiment, Adv. Colloid Interf. Sci. 1 (1967) 111–239, https://doi.org/10.1016/0001-8686(67)80004-6.
[29] H.-Y. Xie, The role of interparticle forces in the fluidization of fine panicles, Powder Technol. 94 (1997) 99–108, https://doi.org/10.1016/S0032-5910(97)03270-1.
[30] J.N. Israelachvili, Intermolecular and Surface Forces, 3rd ed, Elsevier Inc., Amsterdam, 2011, https://doi.org/10.1016/C2009-0-21560-1.
[31] M. Capece, R. Ho, J. Strong, P. Gao, Prediction of powder flow performance using a multi-component granular Bond number, Powder Technol. 286 (2015) 561–571, https://doi.org/10.1016/j.powtec.2015.08.031.
[32] H. Lu, J. Zhong, G.-P. Cao, H.-F. Liu, Gravitational discharge of fine dry powders with asperities from a conical hopper, Part. Technol. Fluid. 64 (2018) 427–436, https://doi.org/10.1002/aic.15954.